

L. Gottardi¹ · H. Akamatsu · M. Bruijn¹ ·
J.-R. Gao^{1,2} · R. den Hartog¹ · R. Hijmering¹ · H. Hoevers¹ · P. Khosropanah¹ · A.
Kozorezov³ · J. van der Kuur¹ · A. van der
Linden¹ · M. Ridder¹

Weak-Link Phenomena in AC-Biased Transition Edge Sensors.

April 5, 2016

Keywords weak-link, Josephson effect, FDM, infra-red detector, SQUID, bolometer, TES, LC resonators

Abstract It has been recently demonstrated that superconducting transition edge-sensors behave as weak-links due to longitudinally induced superconductivity from the leads with higher T_c . In this work we study the implication of this behaviour for TES-based bolometers and microcalorimeter under ac bias. The TESs are read-out at frequencies between 1 and 5MHz by a Frequency Domain Multiplexer based on a linearised two-stage SQUID amplifier and high- Q lithographically made superconducting LC resonators. In particular, we focus on SRON TiAu TES bolometers with a measured dark Noise Equivalent Power of $3.2 \times 10^{-19} \text{W}/\sqrt{\text{Hz}}$ developed for the short wavelength band for the instrument SAFARI on the SPICA telescope.

1 Introduction

Superconducting transition-edge sensors (TESs) are highly sensitive thermometers widely used as radiation detectors over an energy range from near infrared to hard x-ray. TESs can be operated both in the dc and ac bias mode and in both cases the detector response can be modelled in great detail^{1,2}. It has been recently demonstrated that TES-based devices behave as weak-links due to the proximity

1:SRON National Institute for Space Research,
Sorbonnelaan 2, 3584 CA Utrecht, The Netherlands

2: Kavli Institute of NanoScience, Faculty of Applied Sciences,
Delft University of Technology,
Lorentzweg 1, 2628 CJ Delft, The Netherlands

3: Department of Physics, Lancaster University,
LA1 4ER, Lancaster, UK

effect from the superconducting leads³. A detailed experimental investigation of the weak-link effects in dc biased x-ray microcalorimeters is ongoing^{4,5} and a theoretical framework for modelling of the resistive state of a TES under dc bias has been developed⁶. Evidence of weak-link effects in ac biased TES microcalorimeters were reported⁷, but an adequate experimental and theoretical investigation is still missing. In this report we present a detailed characterization of a TES-based low- G bolometer developed for the Short Wavelength Band detector of the instrument SAFARI on board of the Japanese infrared mission SPICA⁸. A comparison between the performance of the TES under dc and ac bias is reported.

2 Experimental set-up

For the ac measurements described below we use a Frequency Domain Multiplexer (FDM) system⁹ working in the frequency range from 1 to 5MHz. The read-out is done using a two-stage SQUID amplifier with on-chip linearization from PTB and high- Q lithographic LC resonators¹⁰. The TES arrays chip is mounted on a copper bracket inside a superconducting Helmholtz coil used to generate a uniform perpendicular magnetic field over the whole pixels array. The external magnetic field is shielded using a Nb can covered by few layers of metallic glass tape.

The device under test is a low- G bolometer based on a Ti/Au (16/60 nm) bi-layer, deposited on a $0.5\mu\text{m}$ thick, $130 \times 70\mu\text{m}^2$ suspended Si_3N_4 island connected to the thermal bath via 4 Si_3N_4 cross-shaped supporting legs that are $2\mu\text{m}$ wide and $400\mu\text{m}$ long. The TES area is $50 \times 50\mu\text{m}^2$. It has a critical temperature of $T_C = 85\text{mK}$, a normal state resistance of $R_N = 98\text{m}\Omega$, a measured $G = 0.27\text{pW/K}$ and a calculated Noise Equivalent Power (NEP) of $2.3 \times 10^{-19}\text{W}/\sqrt{\text{Hz}}$. An 8nm thick Ta absorber with an area of $70 \times 70\mu\text{m}^2$ is deposited close to the TES.

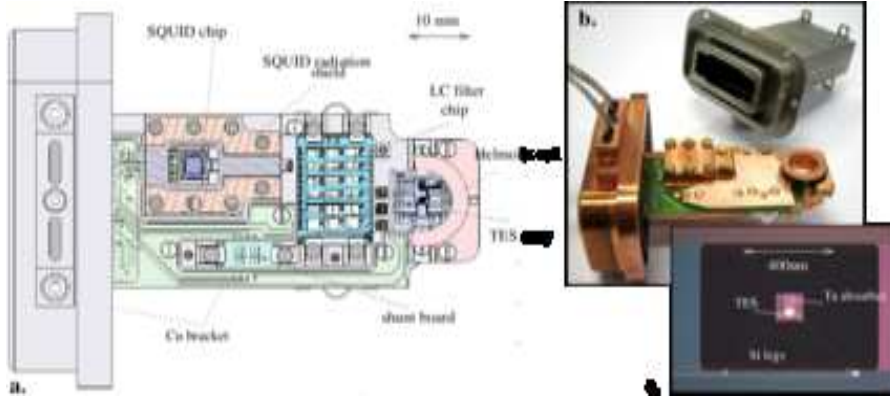


Fig. 1 The schematic drawing (a.) of the Frequency Domain Multiplexer and pictures of the experimental set-up (b.) and the TES bolometer with cross-shaped supporting legs (c.).

The electrical contact to the bolometer is realized by 90nm thick Nb leads deposited on the top of the SiN legs. The sensor was previously characterised under dc bias^{11,12} and showed a power plateau of 9.4fW and a dark NEP of $4.8 \times 10^{-19} \text{W}/\sqrt{\text{Hz}}$ at 30mK. Below we report the results for the TES ac biased at a frequency of 2.4MHz. The FDM set up and a picture of the TES bolometer is shown in Fig. 1.

3 Experimental results

To characterize the detector under ac bias we studied the dependence of the TES current on the voltage, the bath temperature and the applied magnetic field. In Fig. 2 we show the TES current-to-voltage (*IV*) and power-to-voltage (*PV*) characteristics as a function of the bath temperature. The TES current shows regular oscillating structures that are better resolved when looking at the measured power. The maxima of those structures occur at relatively constant TES voltages for all the bath temperatures.

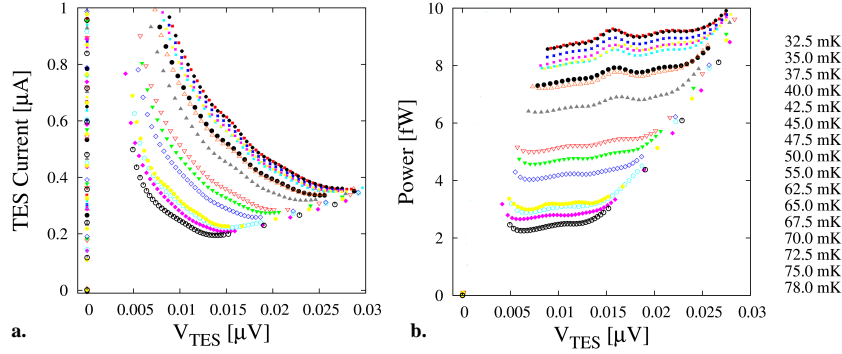


Fig. 2 Measured TES current (a.) and power (b.) as a function of the ac bias voltage for several bath temperature

The dependence of the TES current on the applied magnetic field is shown in Fig. 3. Under ac bias (colored-dotted lines) with the TES in transition we observed a Fraunhofer-like oscillating pattern, typical of a superconducting weak-link structure. Under dc bias (dark line) the current oscillations are generally much smaller and more difficult to see as it was previously reported¹². Another interesting difference between the ac and dc bias measurement is that at large applied magnetic field the ac current does not decrease as one would expect from the Meissner effect. Moreover, a sudden increase of the TES current is observed at certain magnetic fields.

Despite the observed structure in the *IV*'s characteristics the TES bolometer dark NEP at zero magnetic field was measured to be only a factor 1.4 higher than the theoretical value.

In Fig. 4 the dark NEP spectra taken under ac and dc bias at a TES resistance $R_{tes} = 0.3R_N$ and a bath temperature of respectively $T_{bath} = 40\text{mK}$ and $T_{bath} =$

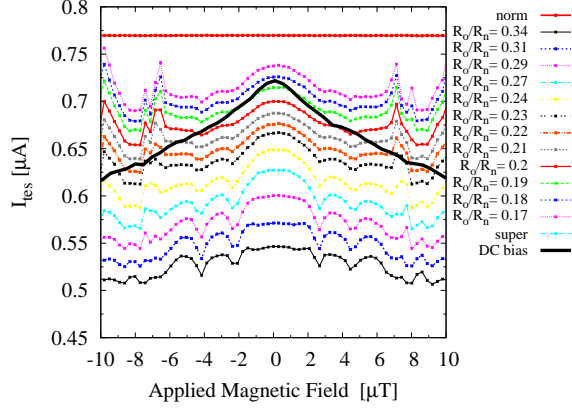


Fig. 3 Measured TES current as a function of applied magnetic field.

20mK are shown. The dark NEP was calculated by dividing the current noise by the responsivity at low frequency, which can be approximated by $\frac{1}{I_O(R_{tes}-Z_{th})}$, where I_O is the effective bias current, R_{tes} is the TES resistance and Z_{th} is the Thevenin impedance in the bias circuit as derived from the calibration of the IV curves.

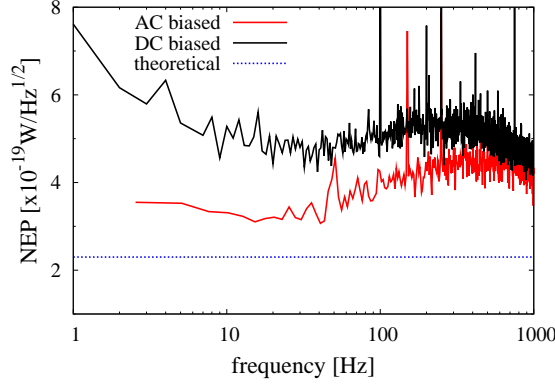


Fig. 4 Measured dark NEP at low frequency under ac and dc bias. The spectra were taken at TES resistance $R_{tes} = 0.3R_N$ and at a bath temperature of $T_{bath} = 40\text{mK}$ and $T_{bath} = 20\text{mK}$ respectively. In the ac bias case a double light-tight box was used.

The dark NEP measured at low frequency ($f \lesssim 40\text{Hz}$) at the optimal bias point in the transition and at zero magnetic field was about $(3.2 \pm 0.13) \times 10^{-19} \text{W}/\sqrt{\text{Hz}}$ and $(4.8 \pm 0.2) \times 10^{-19} \text{W}/\sqrt{\text{Hz}}$ for the ac and dc bias case respectively. The NEP was independent on the bath temperature for temperature approximately below 50mK. The noise measured under ac bias is only 1.4 times higher than the expected theoretical NEP of $2.3 \times 10^{-19} \text{W}/\sqrt{\text{Hz}}$ and was obtained after mounting

the light-tight FDM set-up in a second light-absorbing box. We suspect that even this approach was not sufficient to reduce the effect of the stray radiation to below $10^{-19}\text{W}/\sqrt{\text{Hz}}$ and a further improvement of our experimental set-up is needed.

We remark that the measurements under dc bias were done using a single light-tight box. They are affected at low frequency by an excess of power leaking through the box and by the $1/f$ -noise from the SQUID amplifier.

The observed TES current response reported above are likely due to the weak-link behaviour of the bolometer. A detailed explanation of the Josephson effects in an ac-biased TES will be reported in a following paper. It can be shown that in order to compare the performance of the TES under ac and dc bias, only the current in-phase with the applied voltage should be considered in the ac bias case. The rms value of the in-phase ac current is equivalent to the dc current value measured in a dc biased TES. This has been experimentally verified and the results are shown in Fig 5.a. The current-to-voltage characteristics measured under ac and dc bias

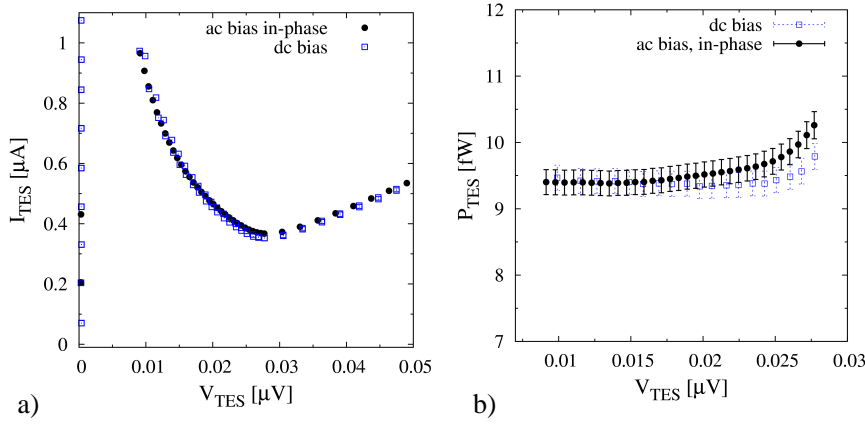


Fig. 5 *IV* (a) and *PV* (b) characteristics of the TES-based bolometer measured under ac and dc bias.

show good agreement within the experimental uncertainties due to the calibration procedure. Under ac bias the quasiparticle current I_{qp} , being in-phase with the applied voltage, is the only current which contributes to the power dissipated in the TES. The data sets plotted in Fig 5.b are the measured *PV* characteristics of the bolometer under ac and dc bias respectively. The *PV* curves are consistent with each other within the calibration errors. We clarify here that the TES current is calibrated using the nominal SQUID parameters and using standard SQUID signal calibration techniques, while to obtain the TES voltage we assumed the TES normal state resistance R_N to be known and performed a linear fit of the superconducting and normal branches of the measured *IV* curves. The TES R_N has been measured on test TiAu structures with 4 points measurements in a dedicated test set-up. The error on R_N is about 1%. This calibration procedure is particularly sensitive to how accurate the normal branch of the *IV* curve has been measured. In both the ac and dc bias case we estimate the total uncertainties to be about 2% and 4% in the current and power respectively.

4 Conclusion

We observed weak-link behaviour in the ac biased TES-based low G bolometer developed for SAFARI. A complete modeling of the weak-link effect in an ac biased detector is under development. When looking only at the current component in-phase with the applied bias voltage the TES current and power response under ac bias is comparable with the dc data. A dark NEP of $(3.2 \pm 0.13) \cdot 10^{-19} \text{W}/\sqrt{\text{Hz}}$ was observed with the pixel ac-biased at 2.4MHz. The measured dark NEP is only a factor of 1.4 higher than the expected theoretical value and is very likely affected by a not yet stray-light free environment.

References

1. D.S. Swetz, D.A. Bennett, K.D. Irwin, D.R. Schmidt, and J.N. Ullom. *Appl. Phys. Lett.*, 101:242603, 2012.
2. J. van der Kuur, L. Gottardi, M.P. Borderias, B. Dirks, P. de Korte, M. Lindeman, P. Khosropanah, R.H. den Hartog, and H. Hoevers. *Applied Superconductivity, IEEE Transactions on*, 21(3):281–284, 2011.
3. J.E. Sadleir, S.J. Smith, S.R. Bandler, J.A. Chervenak, and J.R. Clem. *Phys. Rev. Lett.*, 104:047003, 2010.
4. J.E. Sadleir, S.J. Smith, S.R. Bandler, J.A. Chervenak, and J.R. Clem. *Phys. Rev. B*, 84:184502, 2011.
5. S.J. Smith, J. Adams, C. Bailey, S.R. Bandler, J.A. Chervenak, F. Eckart, M. Finkbeiner, R. Kelley, C. Kilbourne, F. Porter, and J. Sadleir. *J. Low Temp. Phys.*, 167:168, 2012.
6. A. Kozorezov, A. A. Golubov, D.D.E. Martin, P.J. de Korte, M. Lindeman, R.A. Hijmering, J. van der Kuur, H.F.C. Hoevers, L. Gottardi, M.Y. Kupriyanov, and J.K. Wigmore. *Appl. Phys. Lett.*, 99:063503, 2011.
7. L. Gottardi, J. Adams, C. Bailey, S. Bandler, M. Bruijn, J. Chervenak, M. Eckart, F. Finkbeiner, R. den Hartog, H. Hoevers, R. Kelley, C. Kilbourne, P. de Korte, J. van der Kuur, M. Lindeman, F. Porter, J. Sadler, and S. Smith. *J. Low Temp. Phys.*, 167:214–219, 2012.
8. B. Swinyard et al. *In Proc. SPIE Space Telescopes and Instrumentation I: Optical, Infrared, and Millimeter*, 6265(1):62650L, 2006.
9. L. Gottardi, H. Akamatsu, M. Bruijn, J.-R. Gao, R. den Hartog, R. Hijmering, H. Hoevers, P. Khosropanah, P. de Korte, J. van der Kuur, A. van der Linden, M. Lindeman, and M. Ridder. *In Proc. SPIE High Energy, Optical, and Infrared Detectors for Astronomy V*, 8453:845333–1, 2012.
10. L. Gottardi, M. Bruijn, J.-R. Gao, R. den Hartog, R. Hijmering, H. Hoevers, P. Khosropanah, P. de Korte, J. van der Kuur, M. Lindeman, and M. Ridder. *J. Low Temp. Phys.*, 167:161–167, 2012.
11. P. Khosropanah, R. Hijmering, M. Ridder, M. Lindeman, L. Gottardi, M. Bruijn, J. vander Kuur, P. de Korte, J. Gao, and H. Hoevers. *J. Low Temp. Phys.*, 167:188–194, 2012.
12. R. Hijmering, P. Khosropanah, M. Ridder, M. Lindeman, L. Gottardi, M. Bruijn, J. van der Kuur, P. de Korte, J.-R. Gao, H. Hoevers, and B. Jackson. *J. Low Temp. Phys.*, 167:242–247, 2012.